Freeze-Dried Chitosan-Platelet-Rich Plasma Implants for Rotator Cuff Tear Repair: Pilot Ovine Studies

Gabrielle Deprés-Tremblay,[†] Anik Chevrier,[‡] Mark B Hurtig,[§] Martyn Snow,[∥] Scott Rodeo,[⊥] and Michael D Buschmann*,[†,‡]

[†]Biomedical Engineering Institute and [‡]Chemical Engineering Department, Polytechnique Montreal, Montreal, Quebec H3T 1J4, Canada

[§]Department of Clinical Studies, University of Guelph, Guelph, Ontario N1G 2W1, Canada

[∥]The Royal Orthopaedic Hospital, Birmingham B31 2Ap, United Kingdom

[⊥]Sports Medicine and Shoulder Service, The Hospital for Special Surgery, New York, New York 10021, United States

ABSTRACT: Rotator cuff tears are a very common shoulder pathology. Different suturing techniques have been used for surgical cuff repair, but failure of healing remains a significant clinical challenge. The objective of this study was to establish and compare chronic and acute ovine rotator cuff tear models in our laboratory and investigate the feasibility of using chitosan (CS)-platelet-rich plasma (PRP) implants in conjunction with suture anchors to treat rotator cuff tears in large animal models. Repair with suture anchors only was used as control. In two preliminary pilot studies, unilateral full-thickness tears were created in the infraspinatus (ISP) tendon of mature female Texel-cross sheep. In the chronic model ($n = 4$ sheep), the tendons were capped with silicon and allowed to retract for

6 weeks, leading to degenerative changes, whereas the tendons were immediately repaired in the acute model ($n = 4$ sheep). Transected ISP tendons were reattached with suture anchors and, in the case of treated shoulders, implants composed of freeze-dried CS solubilized in autologous PRP were additionally applied to the tendon–bone interface and on top of the repaired site. The chronic defect model induced significant tendon degeneration and retraction, which made repair more challenging than in the acute defect model. Half the tendons in the chronic repair model were found to be irrepairable at 6 weeks. In the other half, the tendons could not be reattached to the footprint due to significant retraction, which made this a model of tissue formation in a gap. In contrast, the acute tendon repair model was executed easily. Extensive bone remodeling and tissue ingrowth at the tendon-bone interface were observed in the case of treatment with anchors + CS-PRP in both models, suggesting that CS-PRP implants could potentially modulate rotator cuff healing processes in large animal models.

KEYWORDS: rotator cuff tear, chitosan, platelet-rich plasma, chronic repair, acute repair, ovine models
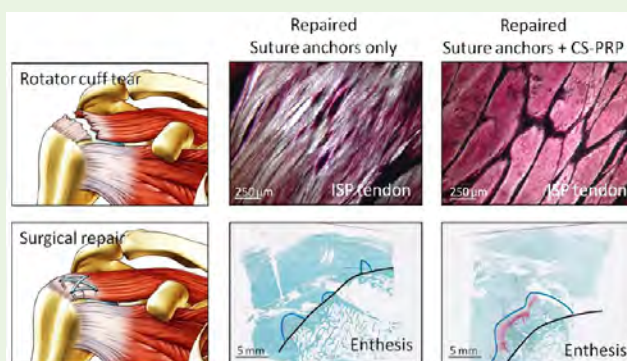
■ INTRODUCTION

Rotator cuff tears are a common cause of morbidity in adults and one of the most common shoulder pathologies.[1,2] Cuff tears are associated with fatty infiltration, muscle atrophy, tendon retraction, and structural and architectural alterations of the musculotendinous unit.[3−5] Ruptures of rotator cuff tendons may eventually lead to irreversible changes in the shoulder, causing chronic pain and severe functional disability. Persistent tendon defects with constant exposure of the intra-articular joint surface and fluid will occur if a rotator cuff tear is not repaired within a certain time frame after injury.[6] It is believed that there may be a "point of no return" in rotator cuff injury, with formation of scar tissue and infiltration of fat, after which the elasticity of the muscle-tendon unit can no longer return to normal.[7]

The goal of rotator cuff repair is to restore the footprint by suturing the tendon directly to the tuberosity using sutures anchors and varying suture configurations with the aim of increasing initial fixation strength, and mechanical stability under cyclic loading.[8] These procedures are assumed to increase footprint contact area and restore normal structure and function of the shoulder,[9] while improving the rate of healing.[10] However, patients often experience failed healing or retears.[11,12] Failure to heal occurs in 20−95% of cases at 2 years following surgical repair,[11,13] depending on surgical treatment used,[14,15] time from injury,[16] tendon quality,[17] muscle quality,[18] biological healing response,[19] patient age, number of tendons involved, and tear size.[20] One limitation of current surgical procedures is that regeneration of the structure and composition of the native enthesis is not achieved following surgical fixation, and

biological augmentation is one possible approach to overcome this limitation.[21]

Growth factors are known to be important in cell chemotaxis, proliferation, matrix synthesis, and cell differentiation,[22] and platelet-rich plasma (PRP) is a readily available source of autologous growth factors. PRP injections have been used clinically to treat rotator cuff tears, since it is believed that increased concentration of platelet-derived growth factors will stimulate revascularization of soft tissue and enhance tendon healing.[20] However, current clinical evidence does not support the routine use of PRP injections to treat rotator cuff tears[23−27] and PRP injections are still very controversial in the orthopedic field. Variability in the isolation protocols and resulting preparations and the poor stability of PRP in vivo are two possible reasons why results have been inconsistent to date.

Chitosan (CS) is a biodegradable polymer that has been used for several tissue repair and regeneration applications. Our laboratory has implemented the use of PRP combined with freeze-dried CS to form injectable implants that coagulate in situ.[28] In vitro release of platelet-derived growth factors is increased and platelet-mediated clot retraction is inhibited by mixing PRP with chitosan.[29] CS-PRP implants were shown to reside for at least 6 weeks subcutaneously in vivo and enhance cell recruitment to surrounding tissues compared to PRP alone.[28,29] CS-PRP implants were tested in ovine meniscus repair models where they increased cell recruitment, vascularization, remodelling and repair tissue integration compared to injection of PRP alone or wrapping the meniscus with a collagen membrane.[30,31] Finally, CS-PRP implants improved marrow-stimulated cartilage repair and induced bone remodeling in a chronic rabbit defect model.[32] We hypothesized that all of the above would also be beneficial to rotator cuff repair, and we subsequently showed in a small rabbit model that CS-PRP implants improve transosseous rotator cuff repair, by favoring tendon attachment through increased bone remodeling.[33]

The two pilot studies presented here used CS-PRP implants in larger sheep rotator cuff repair models. The first study used a chronic repair model, where tendons were allowed to degenerate to a chronic stage prior to repair, while an acute model with immediate repair was used in the second study. In both repair models, the infraspinatus (ISP) tendons were surgically transected and repaired using suture anchors with or without additional application of CS-PRP implants and healing was assessed histologically. Our aim was to establish and compare the larger sheep models in our laboratory and investigate the feasibility of using CS-PRP implants in conjunction with suture anchors for rotator cuff repair in large animal models.

■ MATERIALS AND METHODS

Preparation of Freeze-Dried Chitosan Formulations. Chitosan (degree of deacetylation 80.2%, number-average molar mass M_n 36 000 g/mol, weight-average molar mass M_w 65 000 g/mol,

polydispersity index 1.8) was used to prepare formulations containing 1% (w/v) chitosan, 28 mM HCl, 1% (w/v) trehalose as a lyoprotecting agent (Life Science) and 42.2 mM $CaCl_2$ as a PRP activator (Sigma-Aldrich). Formulations were filter-sterilized and distributed in 1 mL aliquots into sterile, depyrogenized 3 cm³ glass vials for lyophilization using the following steps: 1) ramped freezing to −40 °C in 1 h, isothermal 2 h at −40 °C, 2) −40 °C for 48 h, 3) ramped heating to 30 °C in 12 h, isothermal 6 h at 30 °C, at 100 mTorrs.

Preparation of Platelet-Rich Plasma (PRP). Blood was drawn from the sheep jugular vein immediately prior to surgery. One small tube of blood was drawn for complete blood count and platelet analysis. Then, two 9 mL tubes of blood were collected per sheep and anticoagulated with 1 mL of 3.8% (w/v) sodium citrate each (final citrate concentration 12.9 mM). PRP was extracted with the ACE EZ-PRP benchtop centrifuge. Briefly, the blood was first centrifuged for 10 min at 1300 rpm. The supernatant and first 1−2 mm of erythrocyte sediment was removed and then centrifuged again at 2000 rpm for 10 min. Only the bottom ∼1.5 mL of each tube was retained and resuspended to make PRP, so that ∼3 mL of PRP was extracted per sheep. This isolation method yields a leukocyte-rich PRP (L-PRP) which contained an average of 409 × 10E9/L platelets (2X that of whole blood), 6.2 × 10E9/L leukocytes (1× that of whole blood) and 2.4 × 10E12/L erythrocytes (0.2× that of whole blood).

Experimental Study Design and Surgical Technique. The protocol for this study was approved by the University of Montreal committee "Comité de déontologie de l'expérimentation sur les animaux" (initial date of approval March 10th 2016) and was consistent with the Canadian Council on Animal Care guidelines for the care and use of laboratory animals. Eight adult Texel-cross female sheep (age ranging from 2 to 6 years; weight ranging from 55 to 70 kg) were divided into a chronic repair model group (Table 1) and an acute repair model group (Table 2). In both groups, the surgical method included unilateral exposure of the infraspinatus tendons (ISP) through a muscle separating approach to the lateral aspect of the shoulder using general anesthesia and aseptic technique. The ISP tendon was transected from its original footprint on the humerus, creating a full-thickness rotator cuff tear. The humeral head was debrided with a surgical scalpel removing any tendinous tissue still attached. In both the chronic and acute repair models, the surface of the tuberosity was roughened with use of a curet and the tendon surface slightly abraded prior to anchor insertion.

In the chronic repair model (*n* = 4 sheep; Table 1 and Figure 1), the tendons were capped with a 5 cm silicon tube (3/4 in. wide Penrose drain) to prevent spontaneous reattachment and to allow the tear to degenerate to a chronic stage for 6 weeks. The capped tendons were engulfed in scar tissue after 6 weeks, at the time of the second surgery. After freeing the tendons from scar tissue and removing the silicon tubes, we found that the muscle-tendon unit had significantly retracted, leaving a gap of several centimeters between the end of the tendon and the tuberosity. In two sheep, the ISP tendons were torn as soon as they were pulled to close the gap to the tuberosity, and were found to be irreparable. Therefore, in those 2 sheep, a defect was created in the contralateral shoulders, but this time the ISP tendon was capped with a shorter 5 mm silicon tube and allowed to degenerate to a chronic stage for 2 weeks, without any further attempt to repair. In the third sheep, the 6-week chronic defect was repaired with suture anchors and sutured in a suture bridge configuration using four 4.75 mm PEEK

Table 1. Design of the Chronic Repair Study

sheep no.	treatment right shoulder	treatment left shoulder	necropsy
1	ISP tendon initially left intact; 6 weeks later, tendon transected and capped with 5 mm silicon	ISP tendon transected and capped with 5 cm silicon; 6 weeks later, tendon was found to be irreparable	6 week chronicity + 2 weeks
2	ISP tendon initially left intact; 6 weeks later, tendon transected and capped with 5 mm silicon	ISP tendon transected and capped with 5 cm silicon; 6 weeks later, tendon was found to be irreparable	6 week chronicity + 2 weeks
3	ISP tendon transected and capped with 5 cm silicon; 6 weeks later, tendon repaired with 4 suture anchors	intact control	6 week chronicity + 2 weeks
4	ISP tendon transected and capped with 5 cm silicon; 6 weeks later, tendon repaired with 1 suture anchor + CS-PRP	intact control	6 week chronicity + 2 weeks

Table 2. Design of the Acute Repair Study

| sheep no.	treatment right shoulder	treatment left shoulder	necropsy
1	tendon transected and immediately repaired with 4 suture anchors	intact control	6 weeks
2	intact control	tendon transected and immediately repaired with 4 suture anchors	3 months
3	tendon transected and immediately repaired with 4 suture anchors + CS-PRP	intact control	6 weeks
4	intact control	tendon transected and immediately repaired with 4 suture anchors + CS-PRP	3 months
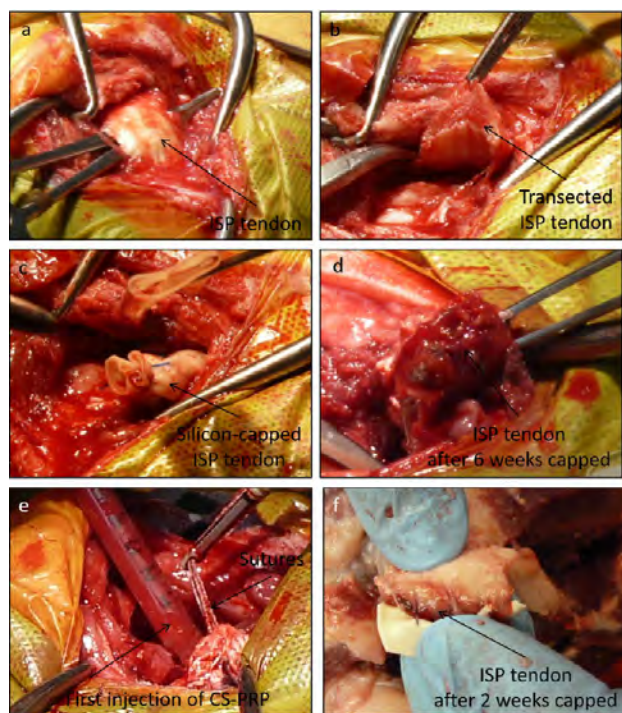
Figure 1. Chronic tear model and repair with CS-PRP. Full-thickness rotator cuff tears were created in the infraspinatus (ISP) tendon of the shoulder (a, b) close to the enthesis and (c) capped with 5 cm length of silicon in 4 sheep. (d) At 6 weeks after surgery, the tendons were macroscopically abnormal and 2 tendons were found to be irreparable. One tendon was repaired with 4 suture anchors in the suture bridge configuration. One tendon was repaired with one suture anchor + CS-PRP. (e) The sutures were preplaced in a Mason-Allen pattern and a first injection of 0.5 mL of CS-PRP was applied at the debrided bone interface. The anchor was inserted to tighten the sutures and an additional 0.5 mL of CS-PRP implant was applied on top of tendon at the repaired site and also under the tendon. (f) Macroscopic appearance of an ISP tendon capped for 2 weeks with 5 mm length of silicon.

Swivelock anchors and 2 mm FiberTape sutures (Arthrex, product no. AR2324-PSLC and AR-7237). In the fourth sheep, the 6-week chronic defect was repaired with one suture anchor with the ISP tendon sutured using a Mason-Allen configuration and the CS-PRP implant was additionally applied in a 2-part manner. Freeze-dried chitosan (1 mL cake) was solubilized with 1 mL of autologous PRP and 0.5 mL of CS-PRP injected at the footprint prior to anchor insertion and then 0.5 mL of CS-PRP was injected on top and under the tendon after reattachment. In both of the above repairable cases, the tendons were too retracted to be reattached at the footprint, hence a gap remained between the tendon and tuberosity after repair, making this a model of tissue formation in a gap. In the 2 sheep where the

degenerated tendons were reattached, the contralateral shoulders were left intact. The animals were allowed to walk ad libitum postoperatively and necropsy was 2 weeks after second surgery (n = 4 sheep).

In the acute repair model (n = 4 sheep; Table 2 and Figure 2), the tendons were transected and immediately repaired with suture anchors
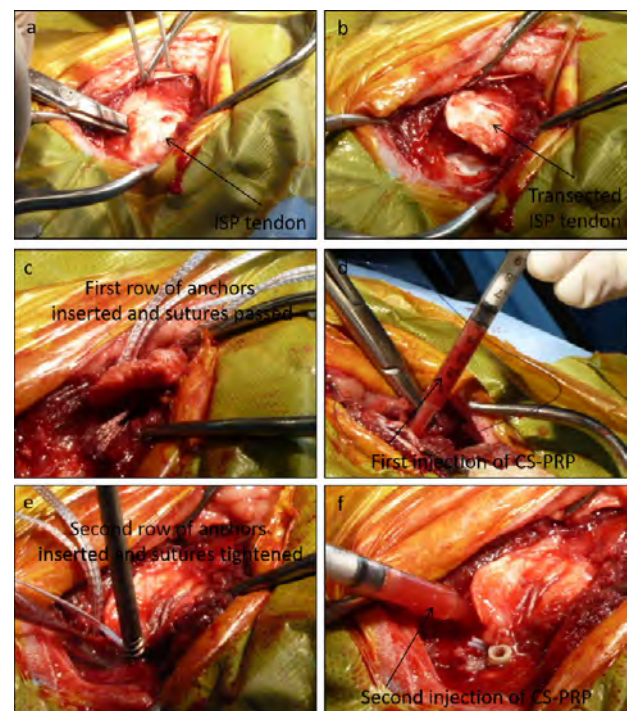

Figure 2. Acute tear model and repair with CS-PRP. (a, b) Full-thickness rotator cuff tears were created in the infraspinatus (ISP) tendon of the shoulder close to the enthesis in 4 sheep. All tendons were immediately repaired with 4 suture anchors in a suture bridge configuration. In 2 out of 4 sheep, repair was augmented with CS-PRP. (c) The first row of anchors were inserted and the sutures were passed and (d) a first injection of 0.5 mL of CS-PRP was applied at the debrided bone interface. (e) The second row of anchors were inserted to tighten the sutures and (f) an additional 0.5 mL CS-PRP was applied on top of tendon at the repaired site and also under the tendon.

and sutured in a suture bridge configuration using four 4.75 mm PEEK Swivelock anchors and 2 mm FiberTape sutures (Arthrex, product no. AR2324-PSLC and AR-7237). In 2 out of 4 sheep, CS-PRP implants were additionally applied in a 2-part manner. The first proximal row of anchors was securely inserted and the sutures were passed through the ISP tendon. Freeze-dried chitosan (1 mL of cake) was solubilized with 1 mL of autologous PRP and 0.5 mL of CS-PRP was injected at the footprint. The sutures were tightened and the second (distal) row of anchors was inserted. Then, 0.5 mL of CS-PRP was injected on top of the repaired site and under the tendon. The animals were allowed to walk ad libitum postoperatively and necropsy was 6 weeks (n = 2 sheep) and 3 months (n = 2 sheep) after repair.

Specimen Collection and Histological Processing. Animals were euthanized by sedation followed by captive bolt pistol. The shoulders were dissected and the humeral head-ISP-tendon unit complex was harvested en bloc from just proximal to the musculotendinous junction. Glenoid surfaces, muscle biopsies and synovial membrane biopsies were collected. All samples were fixed for several days in 10% neutral buffered formalin and trimmed for further processing. The ISP insertion sites, humeral head and glenoid surfaces were decalcified with HCl with trace glutaraldehyde. All samples were dehydrated in graded ethanol series, cleared with xylene and embedded in paraffin. Sections (5 μm thickness) were stained with Safranin O/Fast Green or Hematoxylin and Eosin and scanned with a Nanozoomer RS (Hamamatsu), and images exported using NDP View software

(Hamamatsu) for qualitative histological assessment. In addition, polarized microscopy images of the ISP tendons were obtained with an Axiolab (Zeiss) microscope equipped with a CCD camera (Hitachi HV−F22 Progressive Scan Color 3-CCD).

■ RESULTS

Chronic Repair Model Was More Challenging than the Acute Repair Model. After 6 weeks of chronic degeneration, ISP tendons capped with 5 cm silicon tubes became macroscopically abnormal throughout and were red, spongy (Figure 1d), biomechanically weak, and easily torn. Two of the four tendons were irreparable. Significant retraction had occurred to the extent that the tendons could not be reattached at the anatomic footprint. In the two cases where the tendons were found to be irreparable, a decision was made to operate on the contralateral shoulders, cap the ISP tendons with smaller 5 mm silicon tubes and allow the tears to degenerate to a chronic stage for 2 weeks. Significant retraction and structural abnormalities of the ISP tendon under the capped end were apparent after 2 weeks (Figure 1f), although changes were less severe than in the 6-week chronic model. In both the 6-week capped and the 2-week capped unrepaired defects, abundant scar tissue surrounded the capped ISP tendons and bridged the gap to the tuberosity, which suggests that a robust repair response occurs in this model, even in the presence of a silicon barrier. In contrast to the chronic model, the acute tear model was easily executed and the transected ISP tendons could be reattached at the footprint (Figure 2).

Histological Appearance of ISP Tendons. As expected, intact ISP tendons ($n = 6$ tendons total) consisted of fibrocartilaginous tissue organized in bundles with sparse cells and a small amount of glycosaminoglycans (GAG) (Figures 3a−c and 4a−d). Histologically, none of the test tendons were structurally similar to intact (Figures 3 and 4). Acellular areas were observed in ISP tendons of the chronic defect model, for both the 2-week capped and the 6-week capped, (Figure 3), but not in tendons of the acute model (Figure 4). The 6-week chronic defect repaired with anchors + CS-PRP at 2 weeks ($n = 1$ tendon) had a portion of tendon repair tissue that was rich in polymorphonuclear cells (Figure 3o), and this was not observed in the case of the tendon reattached with suture anchors only ($n = 1$ tendon) (Figure 3j−l). In the acute model repaired with suture anchors only, there was evidence of chondrogenesis within the tendon body at 6 weeks ($n = 1$ tendon) (Figure 4f) and abundant GAG expression at 3 months ($n = 1$ tendon) (Figure 4m), while this was not observed in the case of repair with anchors + CS-PRP ($n = 1$ tendon at 6 weeks and $n = 1$ tendon at 3 months) (Figure 4 i, q). Repaired tendons consisted mainly of disorganized, hypercellular and vascularized tissues (Figures 3 and 4). The one exception was in the case of repair with anchors + CS-PRP at 3 months in the acute model ($n = 1$ tendon), which was mostly organized in bundles and had a portion of repair tissue that was structurally similar to normal tendon (Figure 4q−t), whereas the tendon reattached with suture anchors only ($n = 1$ tendon) had mostly abnormal structural organization (Figure 4m−p). Polarized light microscopy images better highlight the tendon structural organization (Figure 4).

Histological Appearance of the ISP Tendon−Bone Junction. Histologically, none of the repaired insertions had reformed the structure of the native enthesis. In the normal enthesis ($n = 6$ total), the different zones were easily identified and no scar tissue was present above the bone front (Figures 5a−c and 6a−c). The tidemark was still recognizable in the 2-week capped chronic defects ($n = 2$) (Figure 5d), but not in any other group (Figures 5 and 6). In all cases, even in untreated chronic defects (Figure 5d, g), scar tissue was growing superior to the enthesis and integration of the scar tissue with the underlying bone was achieved through bone remodeling and ingrowth at the junction of the scar tissue with the original bone front (Figures 5 and 6). Shoulders treated with anchors + CS-PRP showed extensive bone remodeling and tissue ingrowth at the tendon-bone junction in both the chronic repair model at 2 weeks ($n = 1$ treated with anchors + CS-PRP vs $n = 1$ anchors only) (compare o to l in Figure 5) and the acute repair model at 6 weeks and at 3 months ($n = 1$ treated with anchors + CS-PRP vs $n = 1$ anchors only at each time point) (compare g and m to d and j in Figure 6).
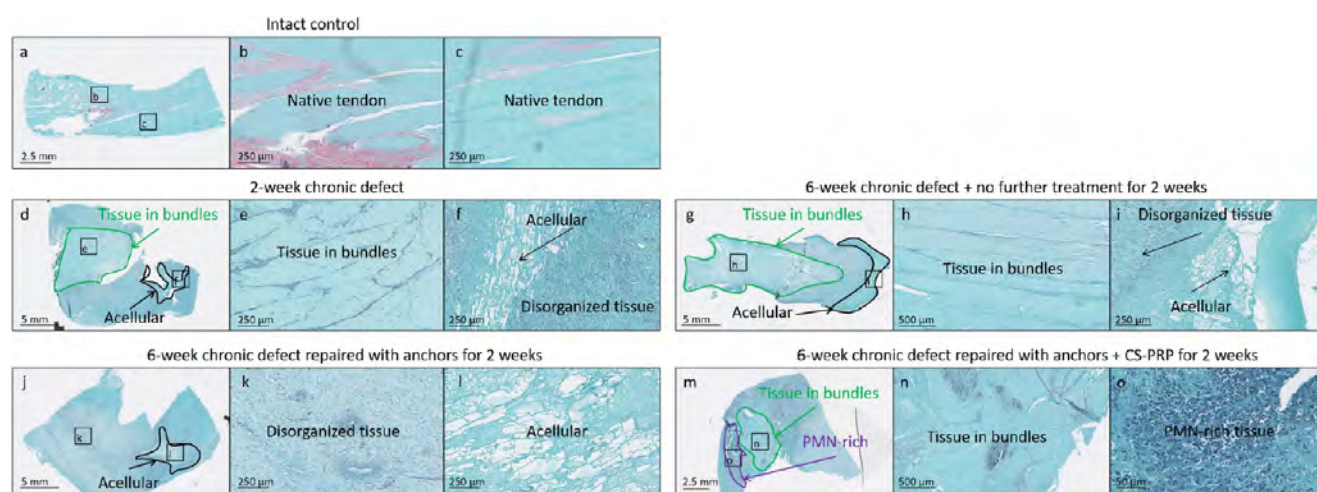

Figure 3. Safranin O/Fast Green stained paraffin sections of the ISP tendons in the chronic repair model. (a−c) Intact control tendons ($n = 2$ tendons) were organized in bundles, as expected. (d−i) Bundle organization was still apparent in areas of untreated tendons at chronic stage, whereas other areas were disorganized, hypercellular, and vascularized or hypocellular. (j−l) The tendon of the shoulder treated for 2 weeks with suture anchors ($n = 1$ tendon) was mostly disorganized, hypercellular, and vascularized, with a small hypocellular area. (m−o) The tendon of the shoulder treated with suture anchors + CS-PRP ($n = 1$ tendon) was mostly disorganized, hypercellular, and vascularized, with a small area organized in bundles and another area rich in polymorphonuclear cells.
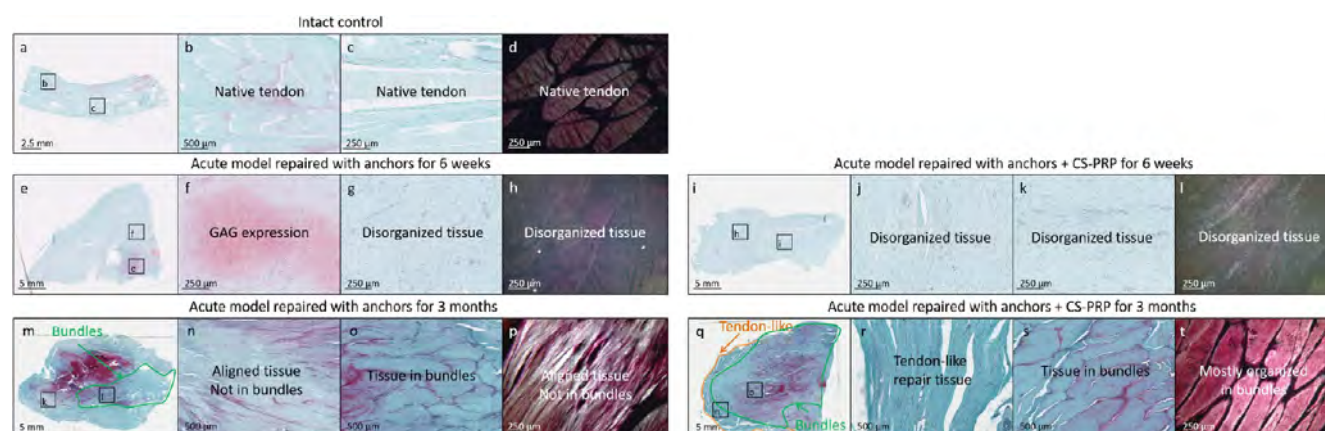
Figure 4. Safranin O/Fast Green-stained paraffin sections and (d, h, l, p, and t) polarized light microscopy images of the ISP tendons in the acute repair model. (a−d) Intact control tendons (n = 4 tendons) were organized in bundles, as expected. (e−l) At 6 weeks postsurgery, the tendons were mostly composed of a disorganized and vascular fibrous repair tissue in both groups. (e, f) Chondrogenesis and GAG expression were apparent in the anchors only group at 6 weeks (n = 1 tendon), but (i, j) this was absent in the tendon treated with anchors + CS-PRP (n = 1 tendon). (m−p) At 3 months postsurgery, the tendon in the anchors only group contained aligned tissue, expressed high levels of GAG, and had only a small area organized in bundles (n = 1 tendon). (q−t) In contrast, the tendon in the anchors + CS-PRP group was mostly organized in bundles with a smaller area of tendon-like repair tissue (n = 1 tendon).
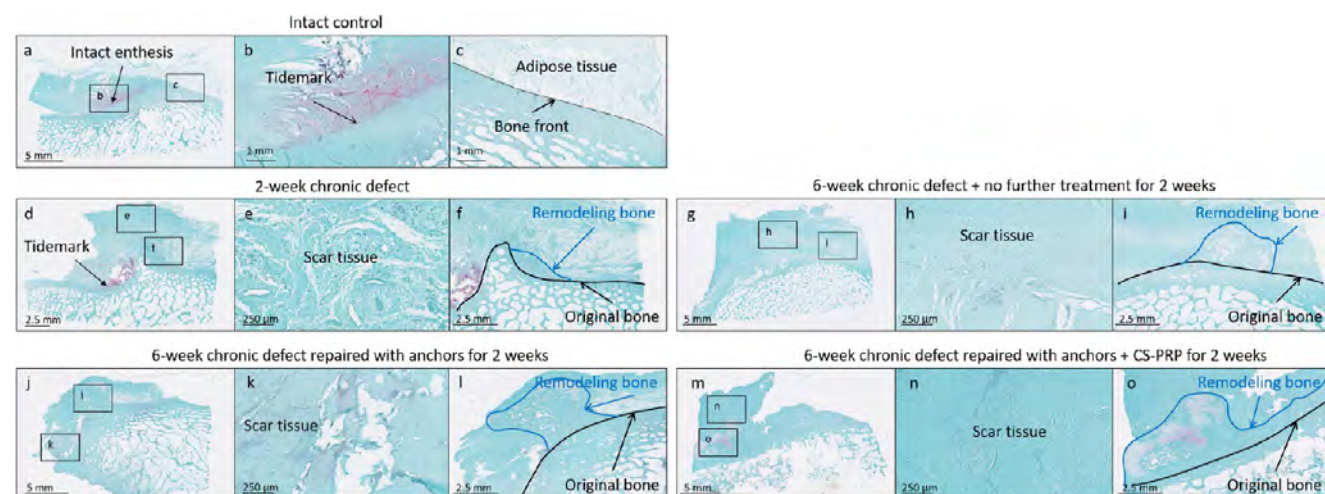

Figure 5. Safranin O/Fast Green-stained paraffin sections of the ISP tendon entheses in the chronic repair model. (a−c) Intact controls (n = 2) had normal entheses consisting of (1) unmineralized fibrocartilage, (2) tidemark, (3) mineralized fibrocartilage, and (4) bone, as expected. (d) The tidemark was still recognizable 2 weeks after defect creation, but (g, j, m) not at longer time points or after repair. (d, g) Scar tissue was growing above the entheses in the untreated chronic defects, suggesting that some spontaneous repair can occur even without any treatment in this model. (f, i, l, o) Integration of the scar tissue with the underlying bone was achieved through bone remodeling and ingrowth into the scar tissue. Treatment with anchors + CS-PRP increased the area of remodeling bone (n = 1) compared to suture anchors only (n = 1) (compare o to l).

Histological Appearance of Other Tissues. In both the chronic and acute repair models, the humeral head was macroscopically free of defects, while small synovial fossae, defined as nonarticulating depressions, were apparent at the center of almost all of the glenoid surfaces. Almost all humeral heads, including intact controls, showed signs of GAG depletion (Figure 7a, c, e, g, and i). Several glenoids, including intact controls, exhibited GAG depletion as well as other structural abnormalities including hypercellularity, cell cloning, and fissures (Figure 7k−m). Muscle histology showed increased fatty infiltration in chronic defects as early as 2 weeks after defect creation, which was not reversed by repair (Figure 8b, c). Similarly, fatty infiltration was also induced by surgical detachment and immediate reattachment in the acute repair model (Figure 8d, e). Histology of the synovial membranes showed that different forms of normal synovium can be found in sheep shoulders including the adipose form of synovium and the fibrous form of synovium (Figure 9). There was mild synovitis and increased cell infiltration in the chronic model treated with anchors + CS-PRP for 2 weeks (Figure 9c), but not in any other sample.

■ DISCUSSION

The purpose of the current study was to establish and compare two large animal models of rotator cuff repair in our laboratory and assess the feasibility of using CS-PRP implants in conjunction with suture anchors for rotator cuff repair. Large animal models, like sheep, have infraspinatus tendons that are similar in size to the human supraspinatus,[34] making them amenable to using repair techniques commonly employed in humans.[6,35] Although these are very preliminary pilot studies, extensive bone remodeling and tissue ingrowth at the tendon-bone junction
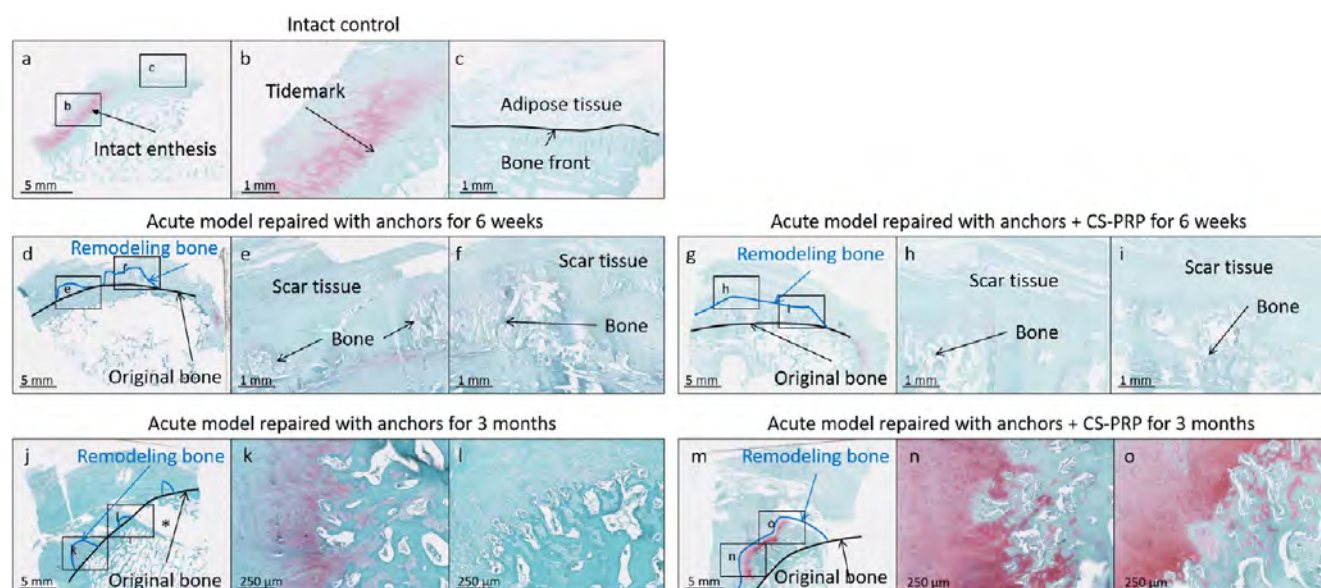
Figure 6. Safranin O/Fast Green-stained paraffin sections of the ISP tendon entheses in the acute repair model. (a−c) Intact controls ($n = 4$) had normal entheses consisting of (1) unmineralized fibrocartilage, (2) tidemark, (3) mineralized fibrocartilage, and (4) bone, as expected. Scar tissue was growing superior to the entheses from (d−i) 6 weeks to (j−o) 3 months postsurgery. (d−o) Integration of the scar tissue with the underlying bone was achieved through bone remodeling and ingrowth into the scar tissue. This was more apparent in the anchors + CS-PRP group compared to the suture anchors only group (compare g and m to d and j) at both 6 weeks and 3 months ($n = 1$ treated with anchors + CS-PRP vs $n = 1$ anchors only at each time point). The site of anchor insertion was apparent in some sections (* in panel j).
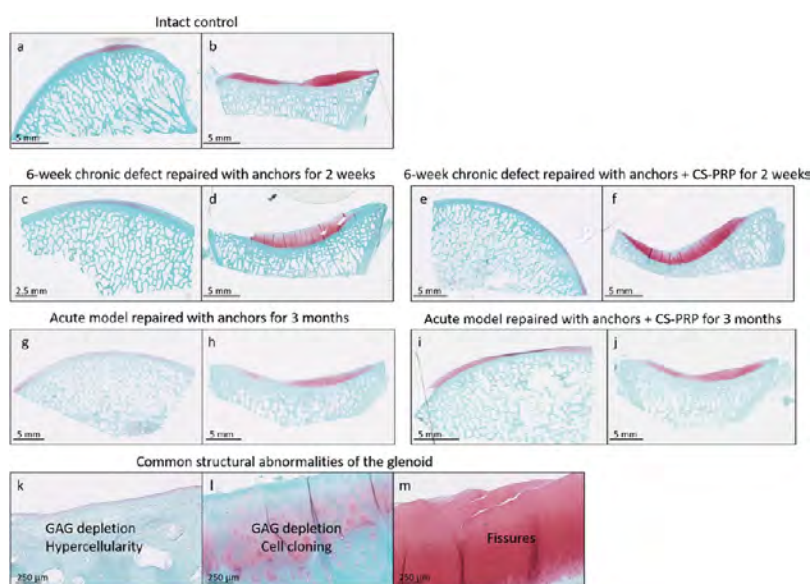

Figure 7. Safranin O/Fast Green-stained sections of humeral head and glenoid articular surfaces (a, b) from intact controls, (c−f) from the chronic defect model, and (g−j) from the acute defect model. (a, c, e, g, and i) The humeral articular surfaces were all structurally normal but showed signs of GAG depletion. (k−m) Mild structural abnormalities were observed at the center of some glenoid articular surfaces, including GAG depletion, hypercellularity, cell cloning, and fissures. These were apparent in all treatment groups as well as the intact controls.

were observed in the case of treatment with anchors + CS-PRP, which suggests that the implants could potentially modulate the healing response in large models of rotator cuff repair.

It seems that chronic animal models would be a better approximation of the clinical situation. However, the sheep exhibits such a robust repair response that it becomes important to actively prevent or minimize spontaneous reattachment in delayed healing models, and this can be achieved by capping the end of the transected tendon. One important finding reported here is the difficulties we faced during implementation of the chronic repair model. We found

that capping the ISP tendons for 6 weeks with 5 cm silicon tubes likely prevented proper nutrient diffusion and led to cell death and severe tendon degeneration, which rendered some tendons irreparable. Although degeneration was not as marked when the tendons were capped for 2 weeks with 5 mm silicon length, reattachment at the footprint would have been difficult to achieve because the tendon−muscle unit had significantly retracted. Therefore, this chronic model would constitute a model of tissue formation in a gap, and not a "true" tendon repair model, and might be more useful to evaluate the use of tendon patches to bridge the gap for example. Capping with
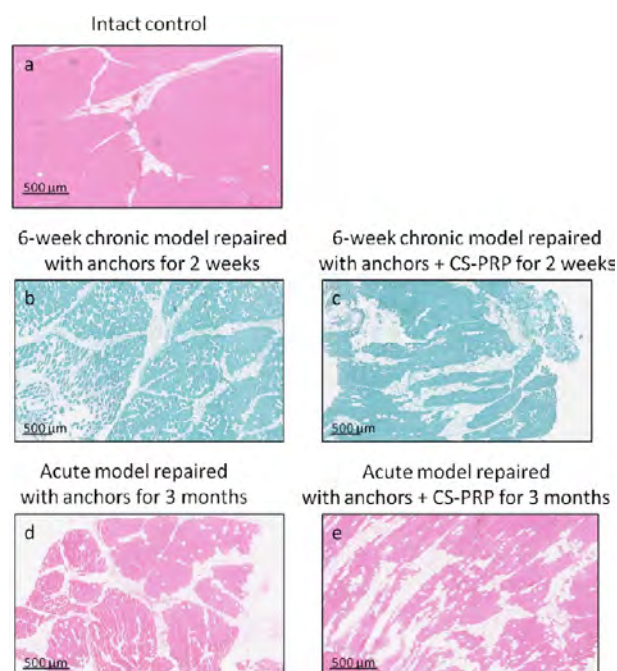
Figure 8. (a, d, e) Hematoxylin and Eosin and (b, c) Safranin O/Fast Green stained paraffin sections of muscle biopsies (a) from intact control, (b, c) from the chronic defect model, and (d, e) from the acute defect model. Fatty infiltration was not prevented by any treatment.
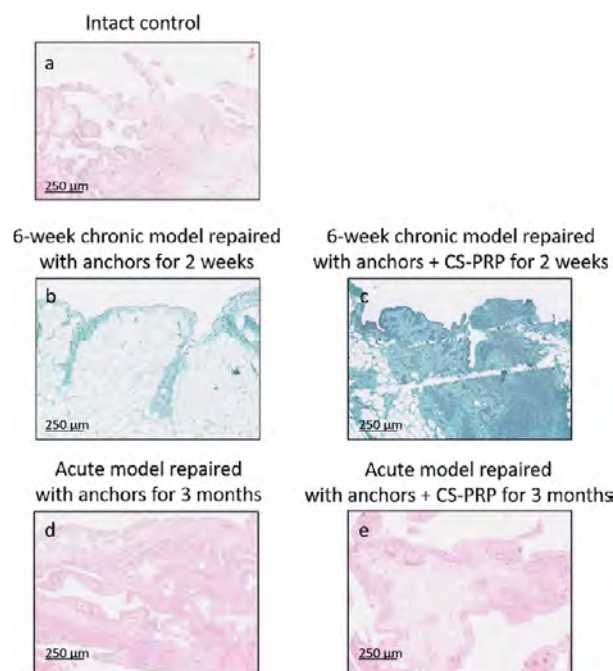

Figure 9. (a, d, e) Hematoxylin and Eosin and (b, c) Safranin O/Fast Green stained paraffin sections of synovial biopsies (a) from intact control, (b, c) from the chronic defect model, and (d, e) from the acute defect model. (c) There was mild synovitis and increased cell infiltration in the chronic model treated with anchors + CS-PRP for 2 weeks.

silicon has been used by other research groups studying chronic rotator cuff repair in sheep, but the surgery usually involves osteotomy, leaving a small bone chip attached to the ISP tendon, with the silicon covering the bone chip and not the tendon itself,[15,36] which may prevent the severe tendon

degeneration that we observed here. This type of tendon release involving an osteotomy has been reported to induce tendon retraction, muscle atrophy, fatty infiltration, and histological changes in the muscle tissue, similar to the clinical situation.[15,36] Other groups have used a preclude sheet to wrap the ISP tendon and allow the tears to develop to chronic stage,[37,38] and tendon retraction and lipid accumulation in the muscle tissue also occur in this model. Preclude is a dura substitute composed of Gore-Tex, with pores of <1 μm in size, which theoretically would still allow nutrient diffusion to the tendons, and most likely would have been a better choice than silicon in the current study. We found that abundant scar tissues bridged the gap between the capped tendon and the tuberosity after 2 weeks and 6 weeks, which supports the notion that the healing response is robust and spontaneous in sheep even in these well-established chronic models.[15,36] Immediate reattachment of a transected tendon does not accurately represent the clinical situation, in which the main challenge resides in aged patients with chronic tears. However, these acute models have become an accepted method of rapidly screening for a treatment's ability to enhance healing.[47] As of now, we consider the acute repair model to be more consistent and easily reproducible.

Even though this study presented some challenges, some interesting findings are worth further discussion. Polymorphonuclear (PMN) cells were observed in the tendon repair tissue of the shoulder treated with anchors + CS-PRP at 2 weeks, but not in the case of suture anchors only. This is not unexpected at this time point, because CS-PRP implants were previously shown to induce PMN recruitment for at least 2 weeks in a rabbit transosseous rotator cuff repair model.[33] PMN were no longer visible at 6 weeks, which suggests that CS-PRP implants were fully degraded by then, which is consistent with previous sheep studies using similar doses of the CS-PRP implants, albeit in the knee joint for meniscus repair.[30,31] Similarly to what was previously seen in the transosseous rotator cuff repair model in the rabbit, the tendon treated with suture anchors alone (nonaugmented) showed chondrogenesis and GAG expression within the tendon body at 6 weeks, while the tendon repair augmented with CS-PRP did not. The significance of chondrogenesis occurring within the tendon repair tissue is still unclear, but we hypothesize that this may be the first step in heterotopic ossification, a well-known complication of tendon injury, which we previously found was inhibited by treatment with CS-PRP implants in the transosseous rabbit model.[33] GAG deposition is also frequently observed in cases of tendonosis.[39,40] The two tendons repaired with anchors + CS-PRP repair technique showed a fairly better tendon structural outcome versus anchors only at 3 months only, with no apparent improvement at 6 weeks, possibly through a modulation of timing of the healing sequence or through increased repair tissue remodeling. These results are preliminary and comparative studies investigating healing at multiple time points would be required to establish the mechanisms of action and the effects of CS-PRP treatment on rotator cuff repair.

During development, tendon-bone integration occurs through establishment of an embryonic tendon-bone attachment unit, which matures into the fibrocartilaginous insertion, known as the enthesis.[41,42] Maturation of the enthesis appears to follow pathways similar to the growth plate development.[41] The insertion site matures through mineralization of fibrocartilage matrix under the influence of chondrocyte-like cells, with associated remodeling through osteoclasts and osteoblasts,

creating the interface between tendon and the tuberosity.[41] Following repair, however, the tendon−bone insertion site usually heals through a fibrovascular scar tissue formation, lacking any sort of reestablishment of the four zones of the native enthesis.[43] Rotator cuff healing occurs in overlapping phases similar to those observed in the case of wound healing, namely the inflammatory phase, the matrix production phase and the remodeling phase.[44] In the chronic and acute models used here, the integration of the tendon repair tissue occurred through bone remodeling and ingrowth at the junction between the tendon and the underlying bone, and the native structure of the enthesis was not re-established. Bone remodeling appears to be a mechanism that enables the repair to become mechanically stronger. It has previously been suggested that strong healing between tendon and the tuberosity, with reformation of a new enthesis, requires bone ingrowth into scar tissue and outer tendon.[45] Other authors have suggested that the formation of a callus appears to be essential for remodelling the tendon-bone boundary after injury.[46] In that respect, it is significant that extensive bone remodeling and tissue ingrowth were observed in the case of treatment with anchors + CS-PRP in both chronic and acute repair models, although it is not possible to draw statistically supported conclusions on the basis of such a small number of samples. Of note, CS-PRP implants have previously been shown to increase bone remodeling over standard treatment in the context of rotator cuff and cartilage repair in small rabbit models, leading to better integration of repair tissues.[32,33]

There were no treatment-specific deleterious effects in the shoulder joint, suggesting that CS-PRP implants have high safety. Structural abnormalities were visible in most glenoids, suggesting that greater stresses are applied on that surface compared to the humeral head in the sheep model. Fatty infiltration of the ISP muscle was induced in both chronic and acute models, and no treatment could reverse that effect. A longer follow-up time may be required to see treatment-specific protective effects. Mild transient synovitis was present in the shoulder treated with anchors + CS-PRP at 2 weeks, but not in the case of suture anchors only, and this was resolved at the later 6 weeks and 3 month time points, once the biomaterial was degraded.

There were several limitations to this study. The main limitation is the small number of animals used, although we feel that these numbers were reasonable for pilot feasibility studies. Obviously, a larger number of animals would be required to draw firm conclusions, and group sizes of 12 animals per treatment are typically used in sheep rotator cuff repair studies.[47] Different repair techniques were used for the chronic group, due to the extensive retraction induced by the silicon capping technique. Furthermore, although the sheep is a commonly used model of rotator cuff repair, it is not identical to human. In contrast to humans, the sheep infraspinatus tendon is not intraarticular, although a bursa exists underneath the tendon. The sheep forelimb is also weight-bearing and has no clavicle, a less-developed acromion, and no coracoacromial arch.[47] Most importantly, robust scar tissue formation occurs between tendon stump and the bone in the sheep, not analogous to humans, where gaping is a common recurrent problem. Inability to control postoperative weight-bearing is another limitation, although these are currently viewed as being difficult to implement in the sheep.[47] Finally, assessment was purely qualitative and, although improved histological appearance

would be expected to translate into superior performance, no other type of measurement was performed.

CONCLUSIONS

In summary, developing techniques to augment of rotator cuff repair remains clinically relevant. The technical challenges associated with the chronic repair model in the sheep make the acute model preferable for future studies. Despite their limitations, these two very preliminary pilot studies suggest that CS-PRP implants could potentially modulate the healing response in large animal models of rotator cuff repair. Future work will involve a larger number of animals and a longer duration of follow-up, with the long-term objective of translating this technology to the clinic.

AUTHOR INFORMATION

Corresponding Author
*E-mail: michael.buschmann@polymtl.ca. Fax: 514 340 2980. Tel: 514 340 4711 ext. 4931.

ORCID
Michael D Buschmann: 0000-0001-7555-8189

Author Contributions
The manuscript was written through contributions of all authors. All authors have given approval to the final version of the manuscript. All authors contributed equally.

Notes
The authors declare the following competing financial interest(s): A.C., M.B.H., and M.D.B. hold shares, M.D.B. is a Director, and M.S. and S.R. are clinical advisors of Ortho Regenerative Technologies Inc.

ABBREVIATIONS

CS   chitosan
PRP   platelet-rich plasma
ISP   infraspinatus
GAG   glycosaminoglycans
PMN   polymorphonuclear

REFERENCES

(1) Lehman, C.; Cuomo, F.; Kummer, F. J.; Zuckerman, J. D. The incidence of full thickness rotator cuff tears in a large cadaveric population. *Bull. Hosp. Jt. Dis.* **1995**, *54* (1), 30−1.
(2) Lippi, G.; Longo, U. G.; Maffulli, N. Genetics and sports. *Br. Med. Bull.* **2010**, *93*, 27−47.
(3) Goutallier, D.; Postel, J. M.; Bernageau, J.; Lavau, L.; Voisin, M. C. Fatty muscle degeneration in cuff ruptures. Pre- and postoperative evaluation by CT scan. *Clin. Orthop. Relat. Res.* **1994**, *304*, 78−83.
(4) Thomazeau, H.; Boukobza, E.; Morcet, N.; Chaperon, J.; Langlais, F. Prediction of rotator cuff repair results by magnetic resonance imaging. *Clin. Orthop. Relat. Res.* **1997**, *344*, 275−283.
(5) Patte, D. Classification of rotator cuff lesions. *Clin. Orthop. Relat. Res.* **1990**, *254*, 81−86.

(6) Derwin, K. A.; Baker, A. R.; Codsi, M. J.; Iannotti, J. P. Assessment of the canine model of rotator cuff injury and repair. *J. Shoulder Elbow Surg* **2007**, *16* (5), 140S–148S.

(7) Laron, D.; Samagh, S. P.; Liu, X.; Kim, H. T.; Feeley, B. T. Muscle degeneration in rotator cuff tears. *J. Shoulder Elbow Surg* **2012**, *21* (2), 164–174.

(8) Cole, B. J.; ElAttrache, N. S.; Anbari, A. Arthroscopic rotator cuff repairs: An anatomic and biomechanical rationale for different suture-anchor repair configurations. *Arthroscopy* **2007**, *23* (6), 662–669.

(9) Di Giacomo, G., Pouliart, N., Costantini, C., De Vita, A. *Atlas of Functional Shoulder Anatomy*; Springer: Rome, 2008.

(10) Denard, P. J.; Burkhart, S. S. The Evolution of Suture Anchors in Arthroscopic Rotator Cuff Repair. *Arthroscopy* **2013**, *29* (9), 1589–1595.

(11) Harryman, D. T., 2nd; Mack, L. A.; Wang, K. Y.; Jackins, S. E.; Richardson, M. L.; Matsen, F. A., 3rd Repairs of the rotator cuff. Correlation of functional results with integrity of the cuff. *J. Bone Joint Surg-Am.* **1991**, *73* (7), 982–9.

(12) Galatz, L. M.; Ball, C. M.; Teefey, S. A.; Middleton, W. D.; Yamaguchi, K. The outcome and repair integrity of completely arthroscopically repaired large and massive rotator cuff tears. *J. Bone Joint Surg-Am.* **2004**, *86* (2), 219–224.

(13) Yamaguchi, K.; Tetro, A. M.; Blam, O.; Evanoff, B. A.; Teefey, S. A.; Middleton, W. D. Natural history of asymptomatic rotator cuff tears: A longitudinal analysis of asymptomatic tears detected sonographically. *J. Shoulder Elbow Surg* **2001**, *10* (3), 199–203.

(14) Iannotti, J. P.; Williams, G. R.; Patel, N. J. Advances in the surgical treatment of disorders of the shoulder. *Surg Annu.* **1994**, *26*, 227–250.

(15) Meyer, D. C.; Hoppeler, H.; von Rechenberg, B.; Gerber, C. A pathomechanical concept explains muscle loss and fatty muscular changes following surgical tendon release. *J. Orthop. Res.* **2004**, *22* (5), 1004–1007.

(16) Bartolozzi, A.; Andreychik, D.; Ahmad, S. Determinants of outcome in the treatment of rotator cuff disease. *Clin. Orthop. Relat. Res.* **1994**, *308*, 90–97.

(17) Riley, G. P.; Harrall, R. L.; Constant, C. R.; Chard, M. D.; Cawston, T. E.; Hazleman, B. L. Tendon degeneration and chronic shoulder pain: changes in the collagen composition of the human rotator cuff tendons in rotator cuff tendinitis. *Ann. Rheum. Dis.* **1994**, *53* (6), 359–66.

(18) Goutallier, D.; Postel, J. M.; Gleyze, P.; Leguilloux, P.; Van Driessche, S. Influence of cuff muscle fatty degeneration on anatomic and functional outcomes after simple suture of full-thickness tears. *J. Shoulder Elbow Surg* **2003**, *12* (6), 550–554.

(19) Shimokado, K.; Raines, E. W.; Madtes, D. K.; Barrett, T. B.; Benditt, E. P.; Ross, R. A significant part of macrophage-derived growth factor consists of at least two forms of PDGF. *Cell* **1985**, *43* (1), 277–286.

(20) Barber, F. A.; Hrnack, S. A.; Snyder, S. J.; Hapa, O. Rotator Cuff Repair Healing Influenced by Platelet-Rich Plasma Construct Augmentation: A Novel Molecular Mechanism Reply. *Arthroscopy* **2011**, *27* (11), 1456–1457.

(21) Després-Tremblay, G.; Chevrier, A.; Snow, M.; Hurtig, M. B.; Rodeo, S.; Buschmann, M. D. Rotator cuff repair: a review of surgical techniques, animal models, and new technologies under development. *J. Shoulder Elbow Surg* **2016**, *25* (12), 2078–2085.

(22) Gulotta, L. V.; Rodeo, S. A. Growth factors for rotator cuff repair. *Clin Sports Med.* **2009**, *28* (1), 13–23.

(23) Vavken, P.; Sadoghi, P.; Palmer, M.; Rosso, C.; Mueller, A. M.; Szoelloesy, G.; Valderrabano, V. Platelet-Rich Plasma Reduces Retear Rates After Arthroscopic Repair of Small- and Medium-Sized Rotator Cuff Tears but Is Not Cost-Effective. *Am. J. Sports Med.* **2015**, *43* (12), 3071–6.

(24) Li, X.; Xu, C.-P.; Hou, Y.-L.; Song, J.-Q.; Cui, Z.; Yu, B. Are Platelet Concentrates an Ideal Biomaterial for Arthroscopic Rotator Cuff Repair? A Meta-analysis of Randomized Controlled Trials. *Arthroscopy* **2014**, *30* (11), 1483–1490.

(25) Zhao, J.-G.; Zhao, L.; Jiang, Y.-X.; Wang, Z.-L.; Wang, J.; Zhang, P. Platelet-Rich Plasma in Arthroscopic Rotator Cuff Repair: A Meta-analysis of Randomized Controlled Trials. *Arthroscopy* **2015**, *31* (1), 125–135.

(26) Warth, R. J.; Dornan, G. J.; James, E. W.; Horan, M. P.; Millett, P. J. Clinical and Structural Outcomes After Arthroscopic Repair of Full-Thickness Rotator Cuff Tears With and Without Platelet-Rich Product Supplementation: A Meta-analysis and Meta-regression. *Arthroscopy* **2015**, *31* (2), 306–320.

(27) Chahal, J.; Van Thiel, G. S.; Mall, N.; Heard, W.; Bach, B. R.; Cole, B. J.; Nicholson, G. P.; Verma, N. N.; Whelan, D. B.; Romeo, A. A. The Role of Platelet-Rich Plasma in Arthroscopic Rotator Cuff Repair: A Systematic Review With Quantitative Synthesis. *Arthroscopy* **2012**, *28* (11), 1718–1727.

(28) Chevrier, A.; Darras, V.; Picard, G.; Nelea, M.; Veilleux, D.; Lavertu, M.; Hoemann, C. D.; Buschman, M. D., Injectable chitosan-platelet-rich plasma (PRP) implants to promote tissue regeneration: In vitro properties, in vivo residence, degradation, cell recruitment and vascularization. *J. Tissue Eng. Regener. Med.* **2017**, in press, DOI: 10.1002/term.2403.

(29) Després-Tremblay, G.; Chevrier, A.; Tran-Khanh, N.; Nelea, M.; Buschmann, M. D., Chitosan inhibits platelet-mediated clot retraction, increases platelet-derived growth factor release, and increases residence time and bioactivity of platelet-rich plasma in vivo. *Biomed. Mater.* **2017**, in press, DOI: 10.1088/1748-605X/aa8469.

(30) Chevrier, A.; Després-Tremblay, G.; Hurtig, M. B.; Buschmann, M. D. Chitosan-platelet-rich plasma implants can be injected into meniscus defects to improve repair. Presented at *2016 Annual Meeting of the Orthopaedic Research Society*; Orlando, FL, March 4–8, 2016; paper no. 0618.

(31) Ghazi zadeh, L.; Chevrier, A.; Hurtig, M. B.; Farr, J.; Rodeo, S.; Hoemann, C. D.; Buschmann, M. D. Freeze-dried chitosan-PRP injectable surgical implants for meniscus repair: results from pilot ovine studies. Presented at *2017 Annual Meeting of the Orthopaedic Research Society*; San Diego, CA, March 19–22 ; Orthopaedic Research Society: Rosemont, IL, 2017; paper no. 2536.

(32) Dwivedi, G.; Chevrier, A.; Hoemann, C. D.; Buschmann, M. D. Freeze dried chitosan/platelet-rich-plasma implants improve marrow stimulated cartilage repair in rabbit chronic defect model. Presented at *2017 Annual Meeting of the Orthopaedic Research Society*; San Diego, CA, March 19–22 ; Orthopaedic Research Society, Rosemont, IL, 2017; paper no. 2282.

(33) Després-Tremblay, G.; Chevrier, A.; Buschmann, M. D. Freeze-dried chitosan-PRP in a rabbit model of rotator cuff repair. Presented at *2017 Annual Meeting of the Orthopaedic Research Society*; San Diego, CA, March 19–22 ; Orthopaedic Research SocietyRosemont, IL, 2017; paper no. 415.

(34) Edelstein, L.; Thomas, S. J.; Soslowsky, L. J. Rotator Cuff Tears: What have we learned from animal models? *J. Musculosk. Neuron Int.* **2011**, *11* (2), 150–162.

(35) Schlegel, T. F.; Hawkins, R. J.; Lewis, C. W.; Turner, A. S. An in vivo comparison of the modified Mason-Allen suture technique versus an inclined horizontal mattress suture technique with regard to tendon-to-bone healing: a biomechanical and histologic study in sheep. *J. Shoulder Elbow Surg* **2007**, *16* (1), 115–21.

(36) Gerber, C.; Meyer, D. C.; Schneeberger, A. G.; Hoppeler, H.; Von Rechenberg, B. Effect of tendon release and delayed repair on the structure of the muscles of the rotator cuff: An experimental study in sheep. *J. Bone Joint Surg-Am.* **2004**, *86* (9), 1973–1982.

(37) Uggen, C.; Dines, J.; McGarry, M.; Grande, D.; Lee, T.; Limpisvasti, O. The effect of recombinant human platelet-derived growth factor BB-coated sutures on rotator cuff healing in a sheep model. *Arthroscopy* **2010**, *26* (11), 1456–62.

(38) Coleman, S. H.; Fealy, S.; Ehteshami, J. R.; MacGillivray, J. D.; Altchek, D. W.; Warren, R. F.; Turner, A. S. Chronic rotator cuff injury and repair model in sheep. *J. Bone Joint Surg-Am.* **2003**, *85* (12), 2391–2402.

(39) DeGiorgi, S.; Saracino, M.; Castagna, A. Degenerative disease in rotator cuff tears: what are the biochemical and histological changes? *Joints* **2014**, *2* (1), 26−28.

(40) Chard, M. D.; Cawston, T. E.; Riley, G. P.; Gresham, G. A.; Hazleman, B. L. Rotator cuff degeneration and lateral epicondylitis: a comparative histological study. *Ann. Rheum. Dis.* **1994**, *53* (1), 30−4.

(41) Thomopoulos, S.; Genin, G. M.; Galatz, L. M. The development and morphogenesis of the tendon-to-bone insertion - What development can teach us about healing. *J. Musculosk. Neuron Int.* **2010**, *10* (1), 35−45.

(42) Zelzer, E.; Blitz, E.; Killian, M. L.; Thomopoulos, S. Tendon-to-bone attachment: from development to maturity. *Birth Defects Res., Part C* **2014**, *102* (1), 101−12.

(43) Apostolakos, J.; Durant, T. J.; Dwyer, C. R.; Russell, R. P.; Weinreb, J. H.; Alaee, F.; Beitzel, K.; McCarthy, M. B.; Cote, M. P.; Mazzocca, A. D. The enthesis: a review of the tendon-to-bone insertion. *Muscles Ligaments Tendons J.* **2014**, *4* (3), 333−342.

(44) Galatz, L. M.., Soft Tissue to Bone Healing in Rotator Cuff Repair. In *Structural Interfaces and Attachments in Biology*; Thomopoulos, S., Birman, V., Genin, G. M., Eds.; Springer Science +Business Media: New York, 2013.

(45) Sanchez Marquez, J. M.; Martínez Díez, J. M.; Barco, R.; Antuña, S. Functional results after arthroscopic repair of massive rotator cuff tears: Influence of the application platelet-rich plasma combined with fibrin. *Rev. Esp Cir Orthop Traumatol* **2011**, *55*, 282−287.

(46) Newsham-West, R.; Nicholson, H.; Walton, M.; Milburn, P. Long-term morphology of a healing bone-tendon interface: a histological observation in the sheep model. *J. Anat.* **2007**, *210* (3), 318−27.

(47) Turner, A. S. Experiences with sheep surgery: Strengths and as an animal model for shoulder shortcomings. *J. Shoulder Elbow Surg* **2007**, *16* (5), 158S−163S.